British Journal of Healthcare and Medical Research - Vol. 12, No. 02
Publication Date: April 25, 2025
DOI:10.14738/bjhr.1202.18387.
Martínez-Hernandez, C. A., Rodríguez-Lelis, J. M., Pérez, O. D., Rodríguez-Ramírez, J. A., Licona, I. L., & Joaquin, P. O. (2025). Application of Continuous Wavelet Transform to Raw Magnetic Resonance Signals to Differentiate Tissue Features. British Journal of Healthcare and Medical Research, Vol - 12(02). 13-26.

Application of Continuous Wavelet Transform to Raw Magnetic Resonance Signals to Differentiate Tissue Features

C. A. Martínez-Hernandez
Departamento de Ingeniería Mecánica,
TECNM/Centro Nacional de Investigación y Desarrollo Tecnológico,
Cuernavaca, Morelos, México

J. M. Rodríguez-Lelis
Departamento de Ingeniería Mecánica,
TECNM/Centro Nacional de Investigación y Desarrollo Tecnológico,
Cuernavaca, Morelos, México

Oscar Domínguez Pérez
Departamento de Ingeniería Mecánica,
TECNM/Centro Nacional de Investigación y Desarrollo Tecnológico,
Cuernavaca, Morelos, México

J. A. Rodríguez-Ramírez
[4]Centro de Investigación en Ingenieía y Ciencias Aplicadas,
Universidad Autónoma de Morelos, Cuernavaca, Morelos, México

Irving Lecona Licona
Departamento de Ingeniería Mecánica,
TECNM/Centro Nacional de Investigación y Desarrollo Tecnológico,
Cuernavaca, Morelos, México

Joaquin, P. O.

ABSTRACT

It is quite useful to diagnose different health conditions such as cancer, osteolysis, amongst others, by the use of images for clinical practice or research. The study and to interpret, anatomical areas of interest has always been a core subject of imaging systems. Technological development in this area has produce had focuses on enhance temporal and spatial resolutions. Although a lot of research has been done to improve images characteristics, the final diagnostic relies on the judgment and experience of the medical specialist since there is not a numerical relationship to the mechanical properties of the human tissues. Based on the former, this work is aimed to develop a procedure to identify the characteristics of tissue and relate them to mechanical properties as an aid to medical diagnosis. Here, the continuous wavelet transform is applied as a passband filter tool to raw magnetic resonance signals. A relation between frequency content and tissues present in the image was identified. From here,it was found that tissue regions exhibiting higher stiffness and toughness emit signals with low frequency, while tissues with lower stiffness and

toughness emit signals with high frequency. The method proposed allows to extract information that can help to generate parameters for classification, detection and mechanical properties of human tissue, for the tissue disease diagnosis.

Keywords: Raw, resonance magnetic signal, filter, mechanical properties, passband filter, tissue.

INTRODUCTION

The magnetic resonance image (MRI) is a noninvasive technique from where the body can be represented through images, that are generated from a radio wave energy, a strong magnetic field, and the atomic-nucleus quantum-mechanical properties of the Hydrogen [1]. The images help to differentiate soft tissue, bone, and some synovial liquids with great clarity. The differentiation is possible by the properties contained on the different tissues present in the body, which depends on their compositions: quantities of lipids, proteins, and water [2-6]. Although clear images are obtained, the interpretation of the images is a function of the medical experiences of the medical specialist.

Nyman et. al. [7] related the mechanical properties of bone with measurement of the free and bound water by nuclear magnetic resonance NMR. Bound water was directly related to bone strength and toughness while free water was inversely related to the modulus of elasticity. Horch et al [8] found that signals of the spectrum 1HNMR are betterthan X-ray to predict yield stress, peak stress, and pre-yield toughness. The 1HNMR signals can be extracted from clinical magnetic resonance MRI, thus offering the potential for improved clinical assessment of fracture risk [8].

A challenge to relate the mechanical properties with the information form the MRI signals is that the acquired RMI signals are saved according to specific data formats, which depends on the vendor. Nowadays, a data sets of raw magnetic resonance signals are available in a standard format, the International Society for Magnetic Resonance in Medicine (ISMRM), proposed a Raw Data Format in 2013. These signals, called ISMRMRD [9]. The MRI signals contain indirect evidence of anatomic, cellular, and atomic features. However, the information into these signals is seldom used for diagnosis and analysis tasks [10].

Many techniques of signal processing have been designed for feature extraction, and time-frequency and multiresolution analysis. The analysis based on the Fourier transform (FT) is the most common, from where the frequency content of the signal is found. Nevertheless, knowledge of the frequency content is not enough for bio-signals due to its non-stationary feature [11]. For analysis of a bio-signals, it is necessary a time-based information for the frequency content. Th e short time Fourier frequency (STFT) is an alternative to achieving the former. However, the fact that the resolution restricted to a preselected window length the analysis becomes limited. Another technique widely used in the signal analysis is the Wavelet Transform (WT). This technique does not require preselected window length and does not have fixed time- frequency resolution over the time-frequency space.

Two types of WT can be recognized the literature, these are discrete wavelet transform DWT and continuous wavelet transform CWT. The DWT is used in denoising, compression, and filter of signals [12–16]. The Continuous Wavelet Transform (CWT) provides a method for displaying

and analyzing characteristics of signals that are dependent on time and scale [12]. The CWT is used as a tool for diagnosis of faults, analysis of responses of a linear mechanical system, feature extraction, detecting and identifying signals with exotic spectral features, transient information content, or other nonstationary properties [17–19].

A key feature of the CWT is that it acts as a passband filter. When the CWT is applied to a signal, the frequency content that occurs at a particular time is extracted. The center frequency and shape of the passband filter is based around the mother wavelet function [20].

Because of the difference in the composition portions of water, proteins and lipids that exist in tissue, we seek determi- nate and compute the relation between the frequencies and its mechanical properties. We used the CWT as a passband filter with the aim to differentiate the frequencies of the diverse tissues present in the resonance magnetic image study.

THEORETICAL FRAMES

Raw Magnetic Resonance Signals

The process of obtain MR signals is shown in Fig.1. Here, the strong magnetic field created by the MRI scanner causes the atoms in a body to align in the same direction of the magnetic field. Radio waves are then sent from the MRI machine and move these atoms out of the original position. As the radio waves are turned off, the atoms return to their original position and send back radio signals. The radio signals are then captured by a receiver transducer, and then stored into a k-space [21].

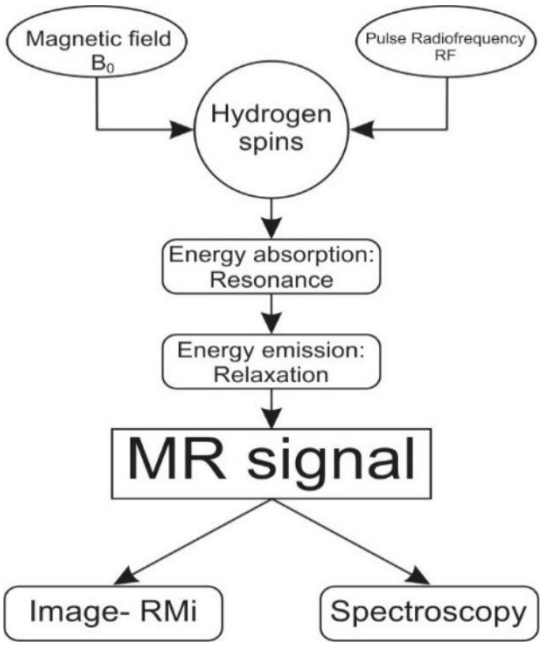

Fig. 1: MR signal schema. The hydrogen spins of the sample are affected by a static magnetic field and a radiofrequency pulse, at Larmor frequency, this allows the energy absorption, later the sample starts to relax and emits energy that is recorded as the resonance magnetic signal, in its frequential domain.

The k-space contains each generated signal by the tissue region of interest. After the excitation pulse has been applied there is a variation of the phase gradient, this information can be saved

URL: http://dx.doi.org/10.14738/bjhr.1202.18387.

into the k-space using the trajectories: Cartesian, Spiral, Radial, and Zig-Zag. The stored signals represent the relationship between the domain frequency and the spin- density signal in time [1, 22, 23]. An example of MR signals acquisition into the k-space using a Cartesian trajectory is shown in the Fig.2.

The International Society for Magnetic Resonance in Medicine (ISMRM) through a subcommittee at 2013, proposed a Raw Data Format, aimed to capture the details of the MRI in a such a way that could allow image reconstruction [24].

The ISMRM Raw Data (ISMRMRD) is structured in two sections: an XML header and the Raw data. The XML section contains all information about acquisition protocol and parameters for image reconstruction. The Raw data is organized as a sequence of data items consisting of fixed-size data headers and the corresponding k-space data for each set of samples or data chunk [24].

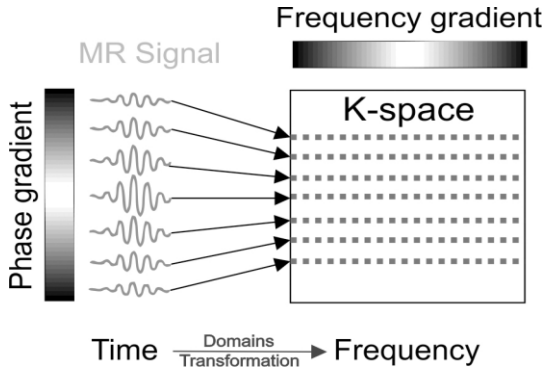

Fig. 2: Example of a raw data matrix, k space, where each transformed signal in the frequency domain is stored into a row of the k space through a Cartesian trajectory.

Tissue Properties

The magnetic resonance imaging uses the variation of the physical properties of tissues, mainly the biochemical composition, to get the images with widely contrasts range. This is because the different tissue properties depend on their composition: lipid portions, proteins, and water [5, 6].

Tissues are formed by similar cells and an extracellular matrix, whose origin is embryonic. They work in combination to develop specialized activities. Many tissues can be grouped by its basic functions or similar morphology, which can be correlated [5]. The mechanical properties are then determined by its composition level. In the elemental level can be found the collagen molecule, which through parallel linking, form the fibrils. These are linked by proteoglycans matrix, which contribute to mechanical behavior too [25].

The contribution of each signal depends besides of the type of tissue to the particular pulse sequence used. As already stated the major contributions sources are water, lipids, small organic molecules, and macromolecules, however the macromolecules cannot be represented by a conventional image from MRI due to their very short T2 value [26]. The behavior of mobile fatty acids is slightly different compared to oxygen-bounded hydrogens in water molecules. Therefore, the interaction between the RF pulse and Larmor frequency in tissues are a function

of the portion of water and fatty content. This phenom is called the chemical shift. As the frequency information is used for spatial encoding, the chemical shift is present over the pixels of the MRI [27].

Continuous Wavelet Transform

The wavelet transform, proposed by Grossman and Morlet [29], is widely used in signal and image processing. The continuous wavelet transform (CWT) is used as a tool for analysis and feature determination. The CWT applied to a signal can be used as filter and to extract the frequency content at a particular time. The transform of signal s(t) at a scale a and at time b, is defined by equation 1. The CWT equation can be solved at a range of scales, a can alter the center frequency and shape of the mother wavelet, to find out different time and frequency information [13].

$$\mathrm{CWT}(a,b) = \frac{1}{\sqrt{|a|}} \int_{-\infty}^{\infty} s(t)\psi^{*}\left(\frac{(t-b)}{a}\right) dt \quad (1)$$

where

- s(t) is the signal in time domain.
- ψ is the wavelet mother.
- a is the scale factor.
- b is the translation factor.
- asterisk $*$ represents the complex conjugate.

the equation 1 is equivalent to convolution of the signal s(t) with an impulse response [13, 20].

The convolution between the signal s(b) and ψ∗(b) implies the presence of a passband filter. Convolution is important because relates three signal of interest: the input signal, the output signal and the impulse response. Convolution describes the procedure to use the impulse decomposition. If the system is considered a filter, the impulse response is called the filter kernel, the convolution kernel or simply, the kernel.

The filtering consists of attenuate o block some frequencies which not are required. The filters with frequency response are classified as (1) High pass filters (2) low pass filters (3) pass- band filters and (4) bandstop filters [28]. In the convolution, is just necessary to know the system's impulse response to calculate what the output will be for any possible input signal [28].

MATERIAL AND METHODS

A Left Tibia (LT) study from Stanford 2D Fast Spin Echo (FSE) project [9] is used in this work. The TL study consists of 28 slices in a sagittal tomographic cut and it was acquired using 16 receiver coils. An example of the slice of LT study is shown in Fig.3.

URL: http://dx.doi.org/10.14738/bjhr.1202.18387.

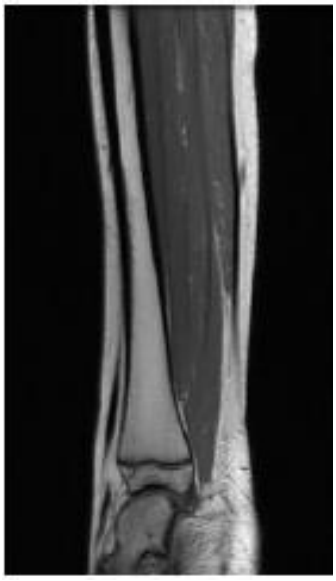

Fig. 3: Left Tibia study, sagittal tomographic cut [9].

Table 1: TL study attributes based on the parameters described in the XML header.

System Field Strength	3.0 T
Receiver Bandwidth (*rBW*)	41.6 KHz
Number of Channels	16
Matrix Size (*Np, Ns, Nsl*)	352 x 202 x 28
Field of View	270.0 mm x 270.0 mm x 4.5 mm
Number of Slices	28
Number of Phases	1
Number of Contrasts	1
Trajectory	Cartesian
Repetition Time	888 ms
Echo Time	9.3 ms
Flip Angle	111◦
Sequence Type	SE

A summary of TL study attributes is described in table 1. The completed description can be found in XML header of the study. From the attributes shown in table 1, where the signal is in the frequency domain, each of then is transformed in the time domain such that a CWT cold be applied. An Inverse Fast Fourier Transform (IFFT) is used to transform between the Frequency to the Time domain of the signal.

In Fig.4 shows the relationship between the signal domain.

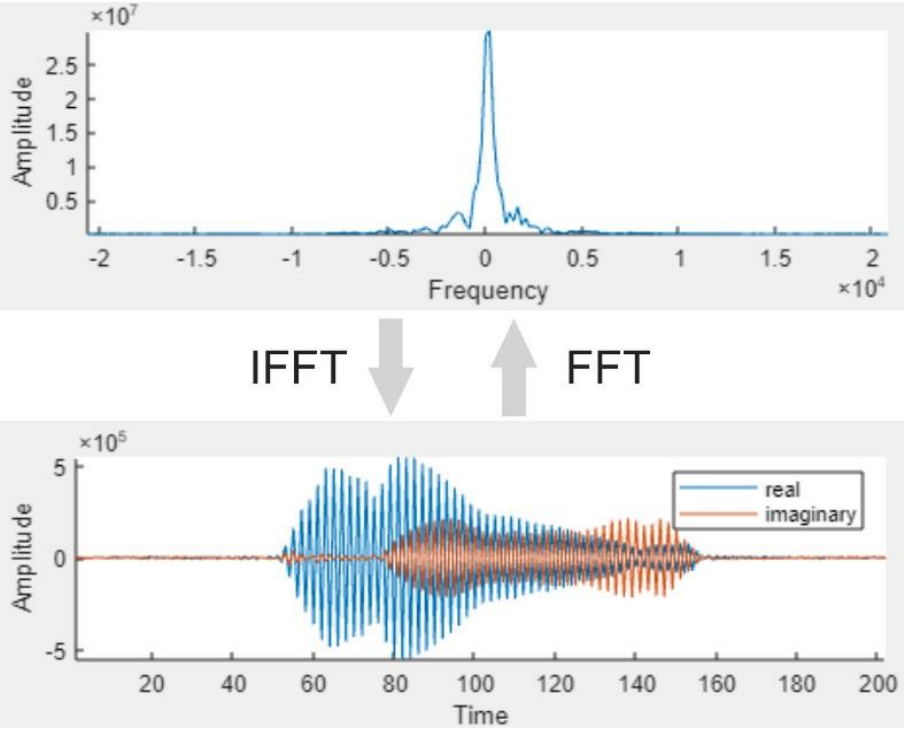

Fig. 4: Example of the relationship between the Frequency and the Time domain, the signal can be transformed using an FFT or IFFT. The signal in the Frequency and the Time domain of TL study [9] and its components, real and imaginary, are shown.

The maximum frequency described by equation 2 and Bandwidth per pixel by equation 3, were computed using the receiver bandwidth (rBW), and signal size (Number of samples, Ns), such that:

$$Fmax = \frac{rBW}{2} \tag{2}$$

$$BWPix = \frac{RBW}{N_s} \tag{3}$$

The CWT implementation is then:

1) In accordance to the application requirements, the mother wavelet is chosen.
2) Determine the scales at which the analysis must be carried out.

In the wavelet analysis, the way in which can be related the scale to frequency is to determine the center frequency of the wavelet, using the following relationship:

$$Fa = \frac{Fc}{a}$$

Where: a is a scale; Fc is the center frequency of the wavelet in Hz.; Fa is the pseudo-frequency corresponding to the scale a, in Hz. From the above relationship, it can be seen, that the scale is inversely proportional to pseudo-frequency, then if one knows the maximum frequency one can compute the minimum scale (amin) as:

URL: http://dx.doi.org/10.14738/bjhr.1202.18387.

$$a_{min} = \frac{Fc}{F_{max}} \quad (5)$$

The CWT and analysis of frequencies are applied to each signal of the k space. After that, one can reconstruct an image using the whole output signals with a particular scale. The analysis is focused on the tissues that are present in the reconstructed image and the frequencies of the signals after using the CWT as a passband filter. Afterwards, the frequency content is analyzed through the Fourier Transform. As was mentioned the advantage of using the CWT as a passband filter is that it helps to identify the moment im which the frequencies are present. This can be used to know the content frequency in each pixel with the aim to relate the energy and the mechanical properties. To understand the influence of frequencies on the pixel the analysis was based on the commutative property of IFFT on 2D. First, we applied the IFFT on 1D over the columns to know the relation between its phases. After, it is applied the step by step the IFFT on 1D over each row, to know what frequency has the maximum value in the spectrum. Then one can compare the maximum value of (Mv) and the final value of (Fv), by the use of the relationship Mv /Fv. If the value of relationships is 1, then the frequency has a maximum influence.

RESULTS

The intervals to be implemented for the CWT analysis are shown in table 2. These intervals were computed according to equations 2 and 3 and table 1. In this work the raw signals of the 11th slice from the Left tibia study [9] are used. The CWT analysis can be supported by scalograms, which are images that allow knowing correlation levels between the wavelet and the signal. In figure 5 the black regions represent the maximum correlation. it can be noted that the correlation occurs near to the maximum frequency, independent of the mother wavelet.

Table 2: Maximum and Minimum scales used according to the mother wavelet used. The difference in the scales is due to each wavelet has a particular center frequency.

Name	Center freq. (Hz)	minimum	maximum
Coiflet	0.7059	1.4118	285.1765
Daubechies	0.6923	1.3846	279.6923
Morlet	0.8125	1.6250	328.2500
Mexican Hat	0.2500	0.5000	101.0000

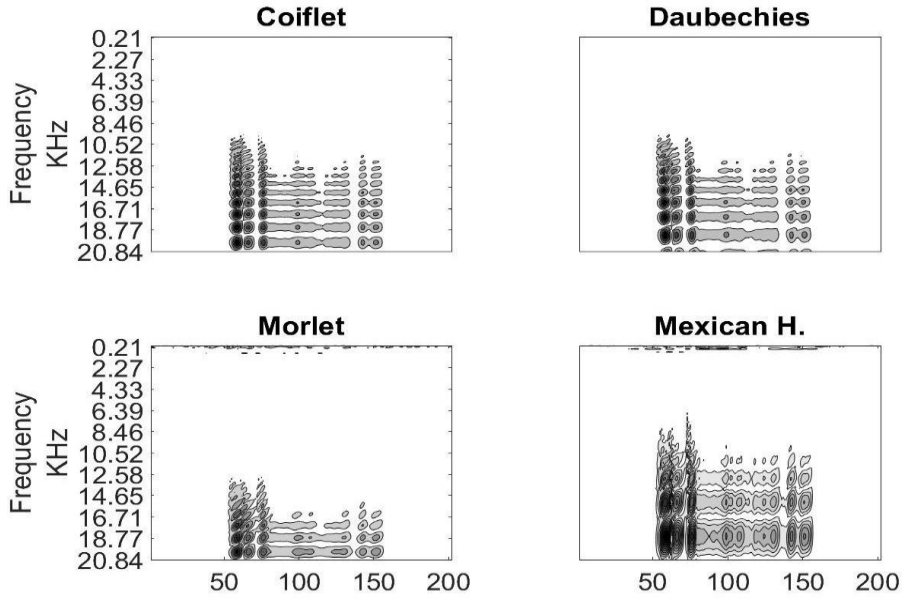

Fig. 5: Generated scalograms using respective scale intervals and its mother wavelet, names of used wavelets are shown.

The aim of this work is to approach the CWT as a passband filter. Therefore, we analyzed the output signal and its frequency content for the raw signals. Using the knowledge a prior, we focused on the regions where there is a maximum level of correlation. From figure 6 it can be observed changes in the frequency content using different scales, in the case of wavelets Coiflet and Mexican hat there is a larger distribution in its frequency content. However, for wavelets Daubechies and Morlet, there are smaller changes in frequency content.

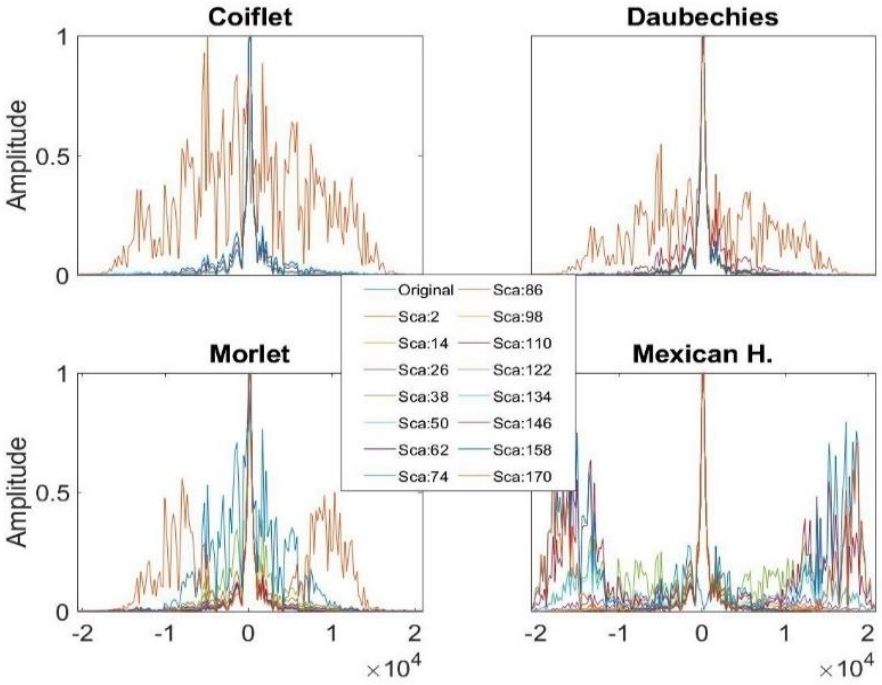

Fig. 6: Distribution of frequency spectrum of signals after to apply CWT using the scale interval and their respective mother wavelet, the name of the wavelet used is shown above the figure.

URL: http://dx.doi.org/10.14738/bjhr.1202.18387.

The changes in frequency content are reflected in each type of tissue. It may be seen in figure 7 a section of the tibia and knee. From left to right are shown the image containing the original data, and the three following the images at 20.73, 16.7 and 10.41.

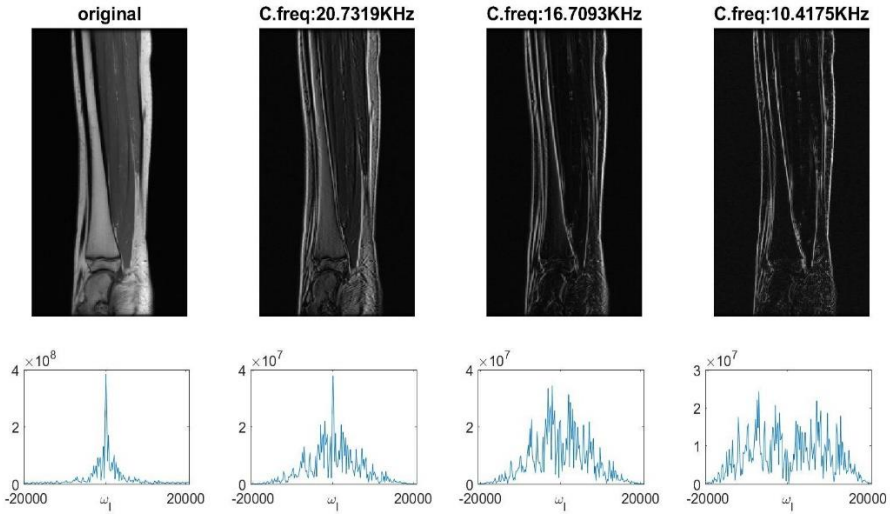

Fig. 7: Comparison between the original image and recon- structed images using Mexican hat wavelet, for different central frequency.

It may be noted that as the central frequency is decreased, the stiffer tissue tends to be defined with more accuracy. First muscular tissue disappears, the cancellus bone, living at the end cortical bone showing the limit of each bone. Because of the signal sampling (signal quadrature), the frequency spectrum is distributed in such a manner that in the center are frequencies near to the Larmor frequency and in extreme are decreasing frequency values, signal quadrature allow identify and distinguish frequencies positive and negative. In figure 8 it can be observed how signals are affected by the CWT. This information is employed to know what frequency affects each pixel on the image.

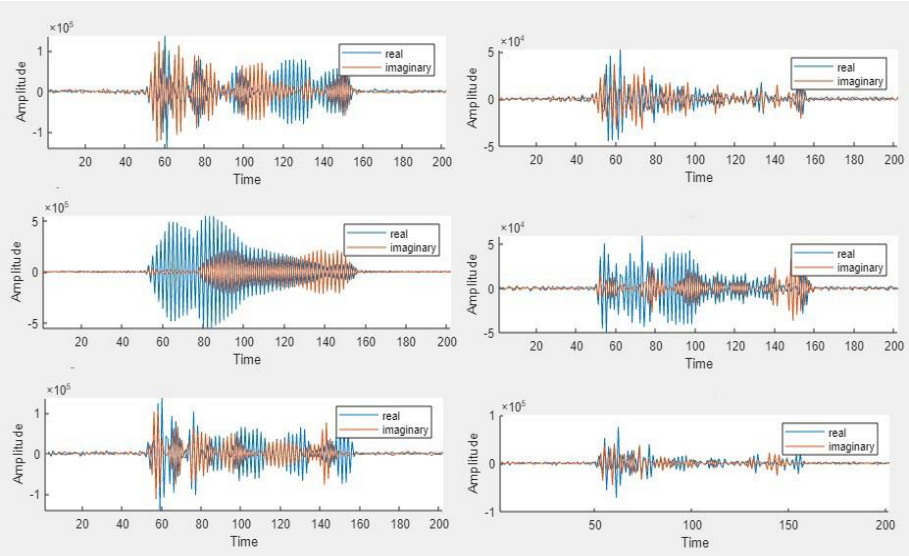

Fig. 8: Comparative between the signal original and decom posed signal using the CWT as a passband filter.

One can reconstruct images using the relationship between the frequency and the percentage of influence in the pixel, as is shown in Fig. 9. Through CWT analysis it can be observed that the relationship between tissues in the image and the frequency content is such that tissues with more strength and toughness emit signals with low frequencies. Here all tissues are influenced by the maximum frequency, because the Larmor frequency is the maximum frequency.

Fig. 9: Reconstructed image using the influences of Larmor frequency ωl, yellow regions indicate the maximum influence and blue regions the minimum influence. The Mexican hat wavelet was used in the analysis.

When the CWT is employed as a filter tool, one can analyze the tissues whose frequency is low respect to ω, in figure 10 it can be noted that tissues with higher strength and toughness. It can be noted in the figure regions of tissue with very strength and toughness as long as the CWT filter allows getting frequencies most low. This is shown the Fig. 11.

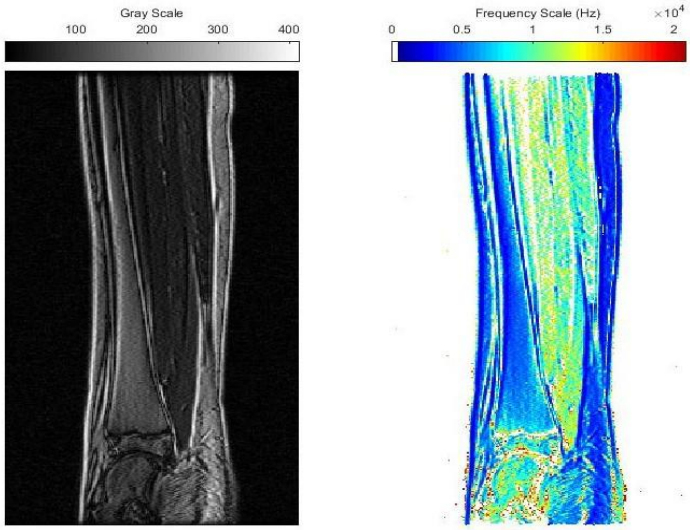

Fig. 10: Reconstructed image using the influences of frequency ωl −5.15 kHz, yellow regions indicate the maximum influence and blue regions the minimum influence. The Mexican hat wavelet was used in the analysis.

URL: http://dx.doi.org/10.14738/bjhr.1202.18387.

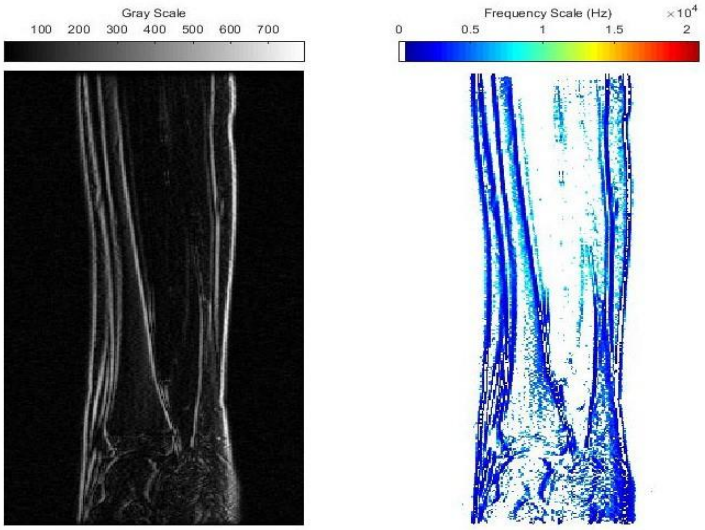

Fig. 11: Reconstructed image using the influences of frequency ωl − 8.87 kHz, navy regions indicate the maximum influence and blue regions the minimum influence. The Mexican hat wavelet was used in the analysis.

DISCUSSIONS

It has been show the use of the CWT as a bass band filter, where the type of tissue can be associated to the central frequency, such that tissues with more stiffness and toughness emit signals with low frequencies and tissue with lower stiffness and toughness to higher frequencies. Here, it can be considered that a span of frequencies can be distinguish for the different types of tissue present and the be associated to mechanical properties.

CONCLUSIONS

A method to analyze the diverse frequencies in a magnetic resonance image by decomposition of raw signals using the CWT as a basspand filter tool is presented. The results showed that tissues or regions with different stiffnes and toughness emit signals as a function of the central frequency, and it can differentiate by using CWT. This method can be used to identify particular frequencies in different studies to relate and quantify the mechanical properties of tissues. Because of the intervals used in CWT depend on the parameters of the study. It is known that the successful CWT application depends on the correct election of the mother wavelet.

ACKNOWLEDGEMENTS

The authors would like to thank to Consejo Nacional de Ciencia y Tecnología (CONACYT), Centro Nacional de Inves tigación y Desarrollo Tecnológico (TECNM/CENIDET) for the support during the realization of this investigation. We also thank Prof. Michael Lustig's group at UC Berkeley and Prof. Shreyas Vasanawala's group at Stanford's Lucile Packard Children's Hospital for the dataset on the website mridata.org.

References

1. Paul C Lauterbur et al. Image formation by induced local inter- actions: Examples employing nuclear magnetic resonance. Nature, 242(5394):190–191, 1973.

2. G Harding, J Kosanetzky, and U Neitzel. X-ray diffraction computed tomography. Medical physics, 14(4):515–525, 1987.

3. Keh-Yang Lee, Jeffrey N Masi, Christian A Sell, Robert Schier, Thomas M Link, Lynne S Steinbach, et al. Computer-aided quantifica- tion of focal cartilage lesions using mri: accuracy and initial arthroscopic comparison. Osteoarthritis and cartilage, 13(8):728–737, 2005.

4. Thorsten M Buzug. Computed tomography: from photon statistics to modern cone-beam CT. Springer Science & Business Media, 2008

5. Robert Lewis Holmes. Living tissues: an introduction to functional histology. Elsevier, 2013.

6. Francis A Duck. Physical properties of tissues: a comprehensive reference book. Academic press, 2013.

7. Jeffry S Nyman, Qingwen Ni, Daniel P Nicolella, and Xiaodu Wang. Measurements of mobile and bound water by nuclear magnetic reso- nance correlate with mechanical properties of bone. Bone, 42(1):193–199, 2008.

8. R Adam Horch, Daniel F Gochberg, Jeffry S Nyman, and Mark D Does. Non-invasive predictors of human cortical bone mechanical properties: T2-discriminated 1h nmr compared with high resolution x-ray. PloS one, 6(1), 2011

9. K Epperson, AM Sawyer, M Lustig, M Alley, M Uecker, P Virtue, et al. Creation of fully sampled mr data repository for compressed sensing of the knee. In SMRT Conf., Salt Lake City, UT, 2013.

10. Curtis P Langlotz, Bibb Allen, Bradley J Erickson, Jayashree Kalpathy- Cramer, Keith Bigelow, Tessa S Cook, et al. A roadmap for foundational research on artificial intelligence in medical imaging: From the 2018 nih/rsna/acr/the academy workshop. Radiology, page 190613, 2019.

11. Dag Stranneby. Digital signal processing and applications. Elsevier, 2004.

12. John Sadowsky. Investigation of signal characteristics using the contin- uous wavelet transform. johns hopkins apl technical digest, 17(3):258– 269, 1996.

13. Lei Nie, Shouguo Wu, Xiangqin Lin, Longzhen Zheng, and Lei Rui. Ap- proximate derivative calculated by using continuous wavelet transform. Journal of chemical information and computer sciences, 42(2):274–283, 2002.

14. Paul S Addison, James Walker, and Rodrigo C Guido. Time–frequency analysis of biosignals. IEEE engineering in medicine and biology magazine, 28(5):14–29, 2009.

15. Hannu Olkkonen. Discrete Wavelet Transforms: Biomedical Applica- tions. BoD–Books on Demand, 2011.Paul S Addison. The illustrated wavelet transform handbook: intro- ductory theory and applications in science, engineering, medicine and finance. CRC press, 2017.

16. Yoon Young Kim and Eung-Hun Kim. Effectiveness of the continuous wavelet transform in the analysis of some dispersive elastic waves. The Journal of the Acoustical Society of America, 110(1):86–94, 2001.

17. Qiao SUN and Ying Tang. Singularity analysis using continuous wavelet transform for bearing fault diagnosis. Mechanical systems and signal processing, 16(6):1025–1041, 2002.

18. J Kilby and H Gholam Hosseini. Extracting effective features of semg using continuous wavelet transform. In 2006 International Conference of the IEEE Engineering in Medicine and Biology Society, pages 1704–1707. IEEE, 2006.

19. Alexander J Casson, David C Yates, Shyam Patel, and Esther Rodriguez- Villegas. An analogue bandpass filter realisation of the continuous wavelet transform. In 2007 29th Annual International Conference of the IEEE Engineering in Medicine and Biology Society, pages 1850–1854. IEEE, 2007.

20. Alberto Del Guerra. Ionizing radiation detectors for medical imaging. World Scientific, 2004

URL: http://dx.doi.org/10.14738/bjhr.1202.18387.

21. Vadim Kuperman. Magnetic resonance imaging: physical principles and applications. Academic Press, 2000.

22. Donald W McRobbie, Elizabeth A Moore, and Martin J Graves. MRI from Picture to Proton. Cambridge university press, 2017.

23. Souheil J Inati, Joseph D Naegele, Nicholas R Zwart, Vinai Roopchans- ingh, Martin J Lizak, David C Hansen, et al. Ismrm raw data format: a proposed standard for mri raw datasets. Magnetic resonance in medicine, 77(1):411–421, 2017.

24. Peter Fratzl. Collagen: structure and mechanics, an introduction. Collagen: structure and mechanics, pages 1–13, 2008.

25. R Adam Horch, John C Gore, and Mark D Does. Origins of the ultrashort-t2 1h nmr signals in myelinated nerve: a direct measure of myelin content? Magnetic resonance in medicine, 66(1):24–31, 2011.

26. W Nitz. Principles of magnetic resonance imaging and magnetic resonance angiography. In Clinical MR Imaging, pages 1–52. Springer, 2006.

27. Steven W Smith et al. The scientist and engineer's guide to digital signal processing. 1997.

28. Alexander Grossmann and Jean Morlet. Decomposition of hardy functions into square integrable wavelets of constant shape. SIAM journal on mathematical analysis, 15(4):723–736, 1984.

29. The HDF Group. Hierarchical Data Format, version 5, 1997-NNNN. https://www.hdfgroup.org/HDF5/.